American Mineralogist, Volume 94, pages 1325–1332, 2009

The crystal structure, origin, and formation of idrialite ($C_{22}H_{14}$): Inferences from the microbeam and bulk analyses

Takuya Echigo,[1,*] Mitsuyoshi Kimata,[1] Teruyuki Maruoka,[2] Masahiro Shimizu,[1] and Norimasa Nishida[3]

[1]Earth Evolution Sciences, Life and Environmental Sciences, University of Tsukuba, Tennoudai 1-1-1, Tsukuba, Ibaraki 305-8572, Japan
[2]Integrative Environmental Sciences, Life and Environmental Sciences, University of Tsukuba, Tennoudai 1-1-1, Tsukuba, Ibaraki 305-8572, Japan
[3]Chemical Analysis Division, Research Facility Center for Science and Technology, University of Tsukuba, Tennoudai 1-1-1, Tsukuba, Ibaraki 305-8572, Japan

Abstract

Idrialite from Skaggs Springs, Sonoma County, California, was studied by microbeam and bulk analyses; the former include micro X-ray diffraction (μ-XRD), electron microprobe (EMP), and micro Fourier transform infrared (μ-FTIR) spectroscopic analyses, and the latter include powder XRD analysis, thermogravimetry-differential thermal analysis (TG-DTA), and carbon isotope analysis. Careful observation under a stereo-microscope clearly disclosed that the examined sample is composed of yellow and brown parts. The yellow parts were identified as idrialite with high crystallinity, whereas the brown ones were confirmed as amorphous matter by μ-XRD. Furthermore, the μ-FTIR spectra revealed that the yellow and brown parts contain hydrophobic and hydrophilic compounds, respectively. EMP analysis showed no chemical zoning and homogeneous distribution of S-bearing molecules in the yellow parts. TG-DTA disclosed that the present idrialite of the yellow part left no residue on heating up to 740 °C; this thermal behavior is similar to that of the other natural organic matter in liquid states such as petroleum and crude oil. The carbon isotopic composition was analyzed using an elemental-analyzer isotopic-ratio mass spectrometer (EA/IRMS). The $\delta^{13}C$ value of the idrialite is –24.429 ± 0.090‰ (vs. V-PDB), which is akin to carbon isotopic compositions of the typical higher-plant triterpenoids contained in sedimentary organic matter.

Both the yellow part (idrialite) and brown part (amorphous organic matter) occur on the coexisting minerals (opalline silica, metacinnabar, and siderite); the textural relationship indicates that the organic matter precipitated after crystallization of the associated minerals. Thus, it is suggested that the organic molecules were migrated by hydrothermal fluids and then separated into hydrophobic (idrialite) and hydrophilic (amorphous organic matter) molecules during the cooling process. Following the separation, idrialite was crystallized and then the amorphous organic matter was precipitated at the final stage of the hydrothermal activity.

Keywords: Idrialite, picene, crystal structure, carbon isotopic composition, polycyclic aromatic hydrocarbons

Introduction

Idrialite, also called curtisite (Wright and Allen 1930), was named and first described by Dumas (1832) from the Idrija mercury deposit in Slovenia (formerly Yugoslavia). The mineral was identified as a molecular crystal of picene ($C_{22}H_{14}$: Fig. 1a, one of polycyclic aromatic hydrocarbons, or PAHs) on the basis of chemical composition, melting point, infrared spectrum, and X-ray powder diffraction pattern (Frank-Kamenetskii and Maleeva 1953; Servos 1965; Strunz and Contag 1965). All these authors concluded the crystal system to be orthorhombic. However, the single-crystal X-ray diffraction study by De et al. (1985) revealed that the crystal structure of highly purified picene is monoclinic.

Geissman et al. (1967) reported that idrialite from Skaggs Springs, Sonoma County, California, consists not only of picene molecules but also chrysene ($C_{18}H_{12}$: Fig. 1b). In addition, idrialite from the same locality contains both N-bearing PAHs (NPAHs) and S-bearing PAHs (SPAHs), as well as PAHs, as confirmed by liquid chromatography-mass spectrometry (LC-MS) analysis (Blumer 1975). Afterward, the applications of both high-resolution gas chromatography-mass spectrometry (GC-MS) and high-performance liquid chromatography (HPLC) by Wise et al. (1986) revealed that idrialite from the same locality consists of five specific PAHs and one SPAH structural series (Fig. 1). Thus, it is reasonable that the incorporation of PAHs other than picene into the crystal structure of idrialite causes the difference in crystal system between idrialite (orthorhombic) and highly purified picene crystals (monoclinic). However, the chemical zoning in idrialite was described by Grinberg and

* Present address: Japan International Research Center for Agricultural Sciences, Ohwashi 1-1, Tsukuba, Ibaraki 305-8686, Japan. E-mail: echigo@jircas.affrc.go.jp

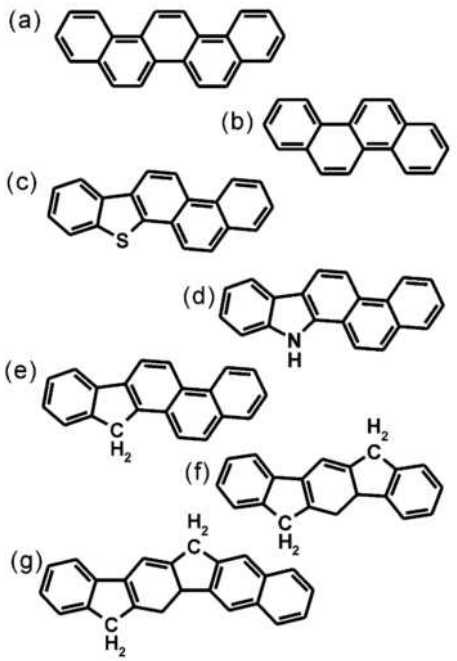

FIGURE 1. Molecular structures of PAHs contained in idrialite from Skaggs Springs. Approximate abundance of their components (Wise et al. 1986) is shown in square brackets: (**a**) picene [40%], (**b**) chrysene [7%], (**c**) benzo-phenanthro-thiophene [10%], (**d**) dibenzo-carbazole [trace], (**e**) dibenzo-fluorene [33%], (**f**) indeno-fluorene [7%], and (**g**) benzo-indeno-fluorene [4%].

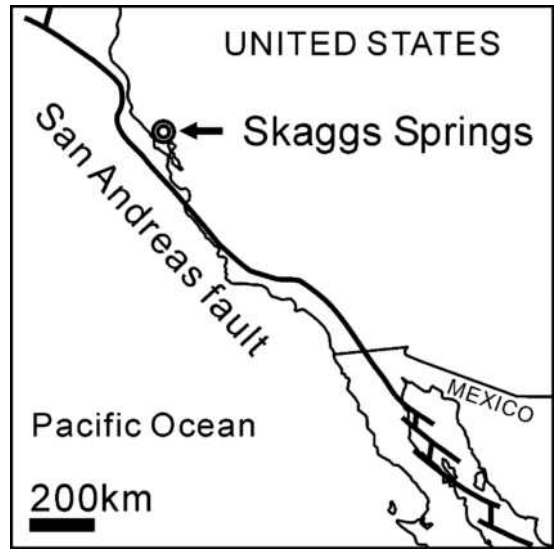

FIGURE 2. Location of Skaggs Springs, Sonoma County, California.

Shimanskii (1954) and hence it was uncertain whether SPAHs and/or NPAHs molecules would exist in the crystal structure of idrialite. Note that the mineral name "curtisite" was used in Grinberg and Shimanskii (1954), Geissman et al. (1967), Blumer (1975), and Wise et al. (1986). The name "curtisite" is discredited since "curtisite" and idrialite are essentially the same mineral species except for the relative amounts of constituent molecules (Gaines et al. 1997).

Here we present the results of in situ microbeam analyses including μ-XRD, EMPA, and μ-FTIR to examine whether SPAHs and/or NPAHs are incorporated into and affect the crystal structure of idrialite from Skaggs Springs. In addition, thermal analysis and carbon isotopic analysis were carried out to elucidate the origin and formation process of the organic mineral.

SAMPLES AND OCCURRENCES

Samples of idrialite were selected from the specimens from Skaggs Springs, Sonoma County, California (Fig. 2), located in the hot spring area of the Franciscan formation (Wright and Allen 1930). The geology of the deposits has been studied in detail (Everhart 1950; Wakabayashi 1992). Skaggs Springs is the first mercury mine yielding commercial quantities of ores (Ransome and Kellogg 1939); the relationship between Hg deposition and organic matter in the West Coast region has been discussed extensively (e.g., Bailey 1959; Vredenburgh 1981; Peabody and Einaudy 1992; Sherlock 2000; Echigo et al. 2007). The mercury deposits in Skaggs Springs lie within a block of interbedded sandstone and shale of Cretaceous age (Everhart 1950). The block is bounded by two northwest-trending faults separating it from rocks of the Franciscan group of Upper Jurassic age (Everhart 1950).

The mineral idrialite occurs as small scattered particles (<1 mm) and the crystalline aggregates along the crack and porous parts in the pale gray and buff sandstone (Figs. 3a and 3b). It is associated with trace amounts of opalline silica ($SiO_2 \cdot nH_2O$), siderite ($FeCO_3$), and metacinnabar (HgS). The idrialite occurs on the surfaces of the associated minerals, which suggests that the organic mineral was precipitated after the crystallization of these inorganic minerals. The paragenesis of the associated minerals was determined by the observation of their spatial distribution (Wright and Allen 1930): opalline silica was first deposited, and siderite and metacinnabar were subsequently crystallized.

The particles included both yellow and brown sections, identified by stereo-microscope (Fig. 3c): the former are platy and aggregated in variable directions, and the latter appear to fill up the spaces between the yellow parts. The yellow and brown sections probably correspond to "curtisite proper" and "curtisitoids" (Grinberg and Shimanskii 1954), respectively. The yellow parts displayed inclined extinction under cross-polarized light, and so were identified as crystalline materials. On the other hand, the lack of transmittance of polarized light through the brown parts suggested that they are amorphous. Although additional observation using a scanning electron microscope was attempted, the brown parts were found to completely evaporate under vacuum, whereas the yellow parts underwent no change. This phenomenon prevented us from analyzing the brown sections with EMPA.

ANALYTICAL METHODS

Microbeam analyses

Micro X-ray diffraction. We employed μ-XRD techniques for individual identification of the materials in the yellow and brown parts (Fig. 3c). The yellow and brown parts were separated carefully under a stereo-microscope and trimmed to equalize their dimensions (100 × 100 × 50 μm). Then each part was attached to a glass fiber, and μ-XRD patterns were obtained using an X-ray microdiffractometer equipped with the crystal movement of Gandolfi-camera style (Kimata et

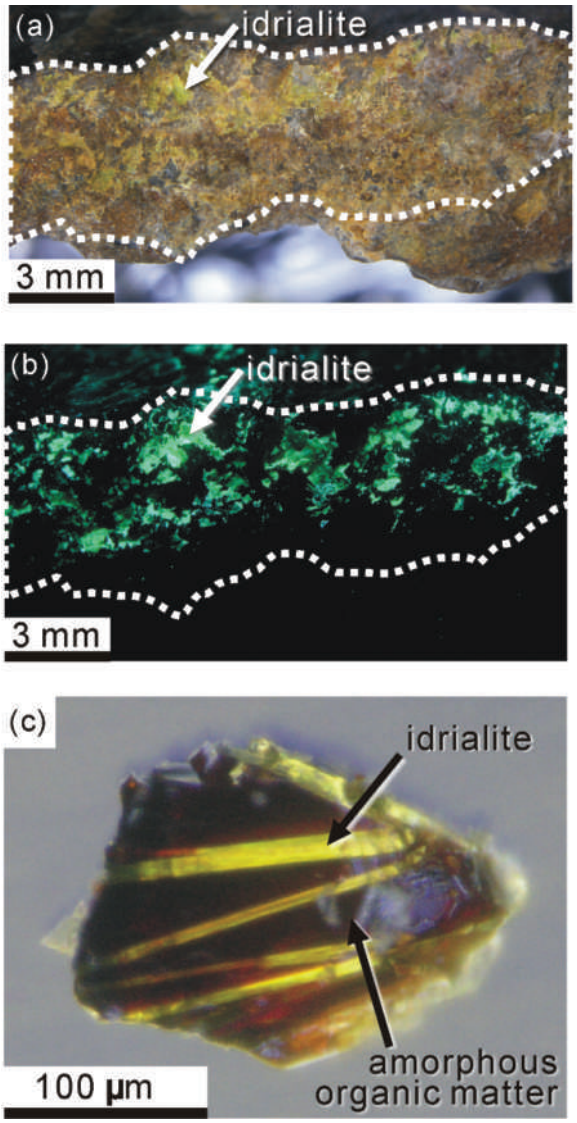

FIGURE 3. Photographs of the present samples from Skaggs Springs. (**a**) Greenish-yellow idrialite crystallized on the fracture of sandstone represented by a white dotted line. (**b**) Idrialite luminescing a brilliant green under ultraviolet irradiation (λ = 365 nm). This mineral crystallized along cracks and partially covers the fracture represented by a white dotted line. (**c**) Microtexture composed of the yellow parts (idrialite crystals) and the brown parts (amorphous organic matters).

al. 1990). The diffractometer has a rotating anode X-ray source (Cr*K*α radiation) and a multichannel detector of position-sensitive proportional counters (PSPC). The XRD analyses were carried out under identical operating conditions (40 kV, 100 mA, and 2 h of exposure time).

Micro infrared spectroscopy. Infrared spectra of the yellow and brown parts were obtained using a Janssen-type micro FTIR spectrometer (JASCO corp.). Each of 10 µm thick particles was chosen from the specimen under a stereomicroscope, and then it was placed on a KBr plate. The transmission spectra were measured in the region of 4000 to 650 cm^{-1}, with 1 cm^{-1} resolution and 400 scans at room temperature in air. A rectangular aperture (100 × 100 µm) was used for the incident beam.

Electron microprobe analysis

Chemical composition of a yellow section was analyzed qualitatively by electron microprobe (EMP), using wavelength dispersive X-ray spectroscopy (WDS) on a JEOL superprobe (JXA-8621). While an EMP analysis of the brown parts was also attempted, they evaporated in vacuum as mentioned above and were found to be unsuitable for the analysis. Analytical conditions for light elements such as C, N, and S followed those described by Nishida and Kimata (1997) and Nishida et al. (2003): 10 µm of beam size, 15 kV of acceleration voltage, and 100 nA of beam current. The crystals used in WD spectrometers were selected as follows: LDE 1 (layered dispersion elements) for analyses of C and N and PET (pentaerythritol) for S (Nishida and Kimata 1997; Nishida et al. 2003).

A small grain of yellow part that has uniform extinction under a polarizing microscope was selected for the EMP analysis to examine whether chemical zoning in the single crystal is observed. Then a back-scattered electron image was obtained and the line analyses were carried out.

Bulk analysis

Acid treatment and mineral separation. To remove inorganic minerals such as carbonates and silicates, acid treatments with mixed acid (HCl:HF = 1:1) were carried out 3 times for 24 h prior to the bulk analyses. This acid treatment was performed in a Teflon dish at room temperature. Following the acid treatment, the samples were washed three times with double-distilled water and dried in air at room temperature. Then the residual inorganic phases such as sulfides and brown parts were completely removed under a stereo-microscope. After the treatments, the samples were analyzed with conventional powder XRD techniques and confirmed to consist of only idrialite (PDF no. 28-2006). Bulk analyses were carried out only for the yellow parts treated as mentioned above, since the brown parts were soluble in the mixed acids and the available sample was insufficient for the analyses described in the following two sections.

Thermal analysis. Thermogravimetric-differential thermal analysis (TG-DTA) was performed with a Thermoplus TG8120 (Rigaku Corp.). The pulverized sample (9.52 mg) was heated in an open platinum crucible at the rate of 10.0 °C/min up to 1000 °C in air, and then two weight-loss steps were observed. Subsequently the same amount of the sample was heated up to 500 °C under the same condition, and then the product was identified by powder XRD.

Carbon isotopic analysis. The isotopic ratio of carbon was measured using an elemental-analyzer isotopic-ratio mass spectrometer (EA/IRMS: IsoPrime EA, GV Instruments Ltd.). The samples wrapped by tin capsules were introduced by an autosampler into the combustion tube heated at 1020 °C with helium gas flowing at 100 mL/min and oxidized by a pulse of oxygen. The combustion tube contained chromium trioxide and silvered cobaltous oxide, which promoted the complete oxidation of carbon species in the sample. The ion signals of CO_2^+ with m/z of 44, 45, and 46 were measured to determine the C isotopic compositions.

The $\delta^{13}C$ values were calculated relative to the carbon isotopic composition of the Vienna-PeeDee Belemnite, V-PDB (latest V-PDB definition; $^{13}C/^{12}C$ = 0.0111802; Zhang and Li 1990; Coplen 1996), in comparison with the analyses of two standards (NBS-19, +1.95‰; IAEA-CO-9, −47.1‰: IAEA AQCS Catalog 1998/1999). The measurements were carried out four times and then the $\delta^{13}C$ and error values were calculated by the method of Maruoka et al. (2003).

RESULTS

Micro X-ray diffraction

The powder XRD patterns of the yellow part, brown part, idrialite (PDF no. 28-2006), and picene (PDF no. 04-0242) were compared (Fig. 4). The pattern of the yellow part (Fig. 4a) closely agrees with that of idrialite (Fig. 4c), although the peak at the lowest angle (2θ = 8.89°) is not indexed by Strunz and Contag (1965, PDF no. 28-2006). The *d*-spacing of the diffraction maximum at the lowest angle (2θ = 8.89°) is 14.77 Å, half of which corresponds to the (004) peak located at 2θ = 17.84° (*d* = 7.38 Å). Thus the peak located at the lowest angle should be attributed to the (002) diffraction of idrialite. In addition, the yellow part showed complete extinction when its section was rotated under crossed polarized light. The observations by µ-XRD and under polarizing microscope revealed that the yellow part is a crystal of idrialite. Hereafter, the yellow part will be referred to as "idrialite."

The XRD pattern of the brown material shows that it consists of both amorphous and crystalline components (Fig. 4b). The

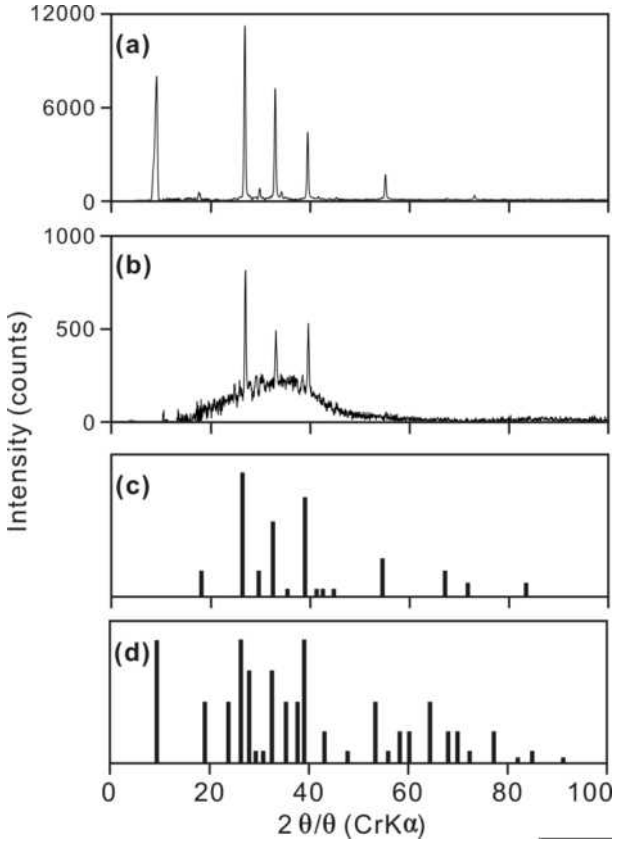

FIGURE 4. Powder X-ray diffraction patterns of (**a**) yellow part, (**b**) brown part, (**c**) idrialite (PDF no. 28-2006), and (**d**) picene (PDF no. 04-0242).

latter was identified as idrialite, judging from the close correspondence of the XRD peaks shown in Figures 4b and 4c. Thus, these peaks are attributed to small idrialite inclusions within the brown material. Considering that the XRD peaks derived from idrialite of the brown part are much smaller than those from the yellow part (single crystal of idrialite), the former part is found to be almost entirely composed of amorphous components.

Electron microprobe analysis

Back-scattered electron images of crystals of the idrialite showed no significant chemical zoning and the line analyses disclosed the homogeneous distributions of sulfur (Fig. 5). Thus the BSE image and line analyses indicate that S-bearing PAH (SPAH) molecules such as benzo-phenanthro-thiophene (Fig. 1c) are homogeneously distributed in the crystal structure of idrialite, although chemical compositions of individual crystals were not examined quantitatively. The characteristic peak of nitrogen located at 3.16 nm (N*K*α: Reed 1997) was not observed in the spectrum (Fig. 6). Thus the concentration of nitrogen-bearing (NPAH) molecules such as dibenzo-carbazole (Fig. 1d) in idrialite crystals is below the detection limit of the present EMP analysis (<1 wt%).

Micro infrared spectroscopy

Figure 7 shows the infrared spectra of synthetic picene (KBr pellet: SDBS-Web 2007), the idrialite (yellow part), the brown

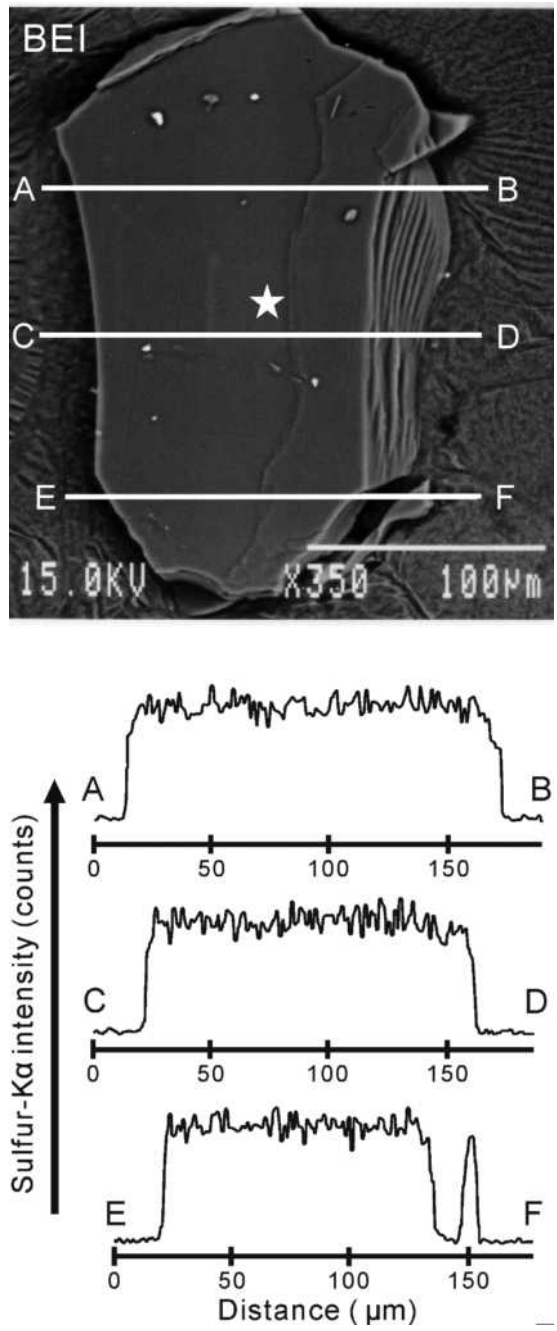

FIGURE 5. Distributions of S along the line AB, CD, and EF in the accompanying back-scattered electron image of idrialite, demonstrating its homogeneity. The white star represents the analytical point yielding the X-ray spectra shown in Figure 6.

part, and synthetic abietic acid (KBr pellet: SDBS-Web 2007). Abietic acid (Appendix 1a) is one of the most typical diterpenes and commonly contained in the resin of higher plants (Standley and Simoneit 1994; Killops and Killops 2005); its relationship with our specimen will be discussed later. The infrared spectra for both synthetic picene (Fig. 7a) and the idrialite (Fig. 7b) are closely similar to each other throughout the range of the measured spectra, whereas the latter shows considerably broadened peaks in the two ranges from 700 to 900 and from 1200 to 1600 cm^{-1}.

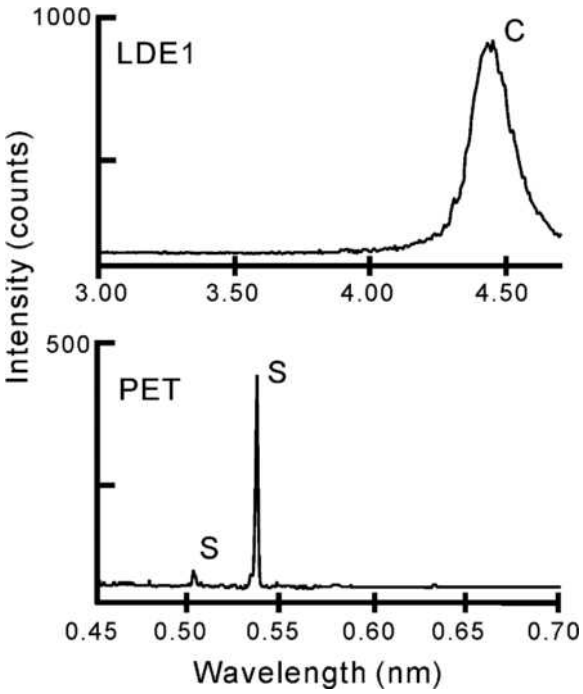

FIGURE 6. X-ray spectra of idrialite shown in Figure 5. The analytical point is as shown in Figure 5a.

The bands within the former range can be assigned to aromatic C-H deformation and the ones within the latter range can be attributed to aromatic C-C stretching (Harwood and Claridge 1997); their broadening may be caused by overlapping of the corresponding peaks derived from various PAHs contained in the crystal structure of idrialite. The peaks located around 2000 cm^{-1} are overtone absorptions of C-H bands (Silverstein et al. 1981).

Comparing the spectrum of synthetic picene (Fig. 7a) with that of the idrialite (Fig. 7b), a sharp peak around 3500 cm^{-1} is a distinctive feature of the latter. This peak may be assigned to N-H stretching (Silverstein et al. 1981), although the N-H stretching band generally occurs around 3350 cm^{-1} due to an intermolecular interaction inherent in a solid (Harwood and Claridge 1997). The increase in the wavenumber results from the lack of the intermolecular interaction between the NPAH molecules (Silverstein et al. 1981), which suggests that NPAH molecules are incorporated into the crystal structure of the present idrialite with extremely low concentration. In addition, the N-H stretching band is sharpened as the concentration is decreased (Harwood and Claridge 1997). Thus, both increasing of the wavenumber and sharpening of the N-H stretching band are consistent with the fact that the N content is below the detection limit of the EMP analysis. Frank et al. (2007) and Jehlička et al. (2006) reported the Raman spectrum of idrialite from Idrija (Slovenia) and also mentioned the presence of N-H in its crystal structure. Thus it is a characteristic common to idrialites from Idrija and Skaggs Springs that trace quantities of NPAH molecules are incorporated into their crystal structures.

The brown part (Fig. 7c) is similar in IR spectrum to the idrialite (Fig. 7b), although both the aromatic C-H deformation bands (700–900 cm^{-1}) and aromatic C-C stretching bands (1200–1600 cm^{-1}) of the former are much broader than those of the latter. The most noticeable differences between these two spectra lie in the relatively broad peaks around 1700 and 2900–3500 cm^{-1} (Fig. 7b). The former is assigned to C=O stretching band and the latter to O-H stretching band (Harwood and Claridge 1997), and thus it is revealed that the brown part contains hydrophilic molecules. In addition, C-H bands between 2900 and 3000 cm^{-1} are more intense than those between 3000–3100 cm^{-1} (Fig. 7c). The former are assigned to non-aromatic C-H and the latter to aromatic C-H bands, respectively (Harwood and Claridge 1997). These assignments suggest that the brown part contains smaller PAH molecules such as diterpenoids. Diterpenoids are one of the most typical and stable biomolecules and commonly used as biomarkers in sediments (Killops and Killops 2005). The molecular structure of abietic acid ($C_{20}H_{30}O_2$) is shown in Appendix 1a as a typical example of diterpenoids. These interpretations are consistent with the observation by Grinberg and Shimanskii (1954) that "curtisite proper" consists of aromatic compounds and "curtisitoids" are rich in oxygen.

Thermal analysis

The TG and DTA curves of the present idrialite are shown in Figure 8. The former displays two steps of weight loss (Fig. 8a) and the latter shows two prominent peaks indicative of exothermal reactions (Fig. 8b). Both weight-loss reactions are accompanied with exothermal reactions, revealing that they are due to combustion reactions (Nakata et al. 1989). The first reaction observed between 200 and 440 °C is attributed to thermal decomposition yielding residual carbonaceous material; similar reactions have been observed in the thermal analyses of coal (Gold 1980) and oil shale (Sonibare et al. 2005). The pyrolysate in the first reaction, a black and brittle product, was analyzed by powder XRD. The diffraction patterns of both the present idrialite before the thermal analysis and the pyrolysate heated up to 500 °C are shown in Figure 9. These patterns indicate that the idrialite before the thermal analysis had high crystallinity and the pyrolysate was amorphous (Fig. 9). The difference in relative intensity between micro and bulk XRD patterns of the present idrialite is attributed to the preferred orientation effect. The present idrialite has a well-developed plate-like cleavage parallel to the basal plane (Fig. 5), and thus the (002) diffraction of the powder XRD (Fig. 9a) is found to be more intense than that of the μ-XRD (Fig. 4a).

The sharp peak around 530 °C in the DTA curve (Fig. 8b) may be ascribed to polymerization of small molecules contained within the pyrolysate in the first reaction; the polymerization reaction is generally observed as an exothermic peak in the DTA curve (Murphy 1970). The second reaction observed between 500 and 740 °C left no residue, thus being attributed to complete combustion (Fig. 8a).

Carbon isotopic analysis

Carbon isotopic composition of the present idrialite is –24.429 ± 0.090‰ (vs. Vienna-PeeDee Belemnite); this $\delta^{13}C$ value is typical of sedimentary organic matter of plant origin (Deines 1980; Galimov 1995). Thus the PAH molecules composing the present idrialite are inferred to have originated from sedimentary organic matter.

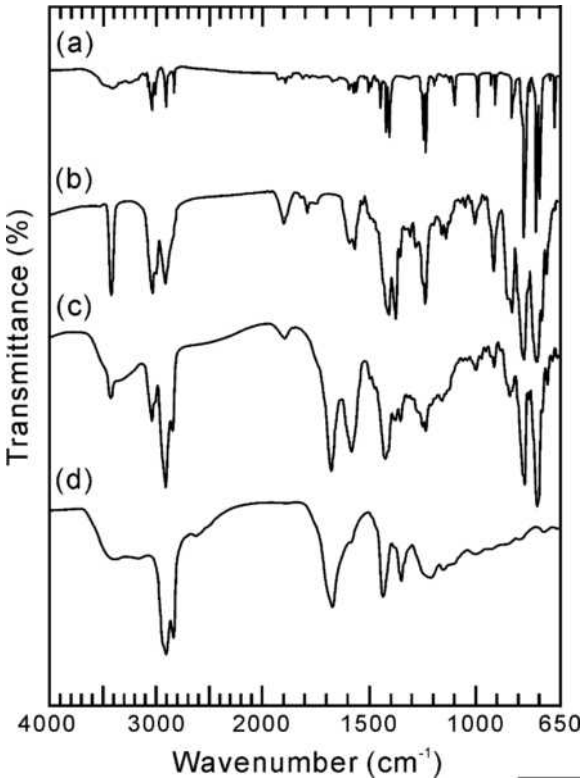

FIGURE 7. Infrared spectra of (**a**) synthetic picene in KBr pellet, (**b**) the yellow part (idrialite crystal), (**c**) the brown part (amorphous organic matters), and (**d**) synthetic abietic acid in KBr pellet.

DISCUSSION

The crystal structure inferred from the microbeam analyses

The microbeam analyses revealed that the PAH, SPAH, and NPAH molecules are incorporated into the crystal structure of the Skaggs Springs idrialite and imply that arrangement of those molecules in the crystal structure is schematically represented as shown in Figure 10. This interpretation is consistent with the following observations: the PAH, SPAH, and NPAH molecules that compose the crystal structure of idrialite have such similar structures that they have been observed to co-crystallize (Jehlička et al. 2006; Echigo et al. 2007). The various PAH molecules including SPAH, NPAH, and picene-like molecules are homogeneously distributed over the crystal structure of idrialite, of which the crystal system (orthorhombic) is different from that of a highly purified crystal of picene (monoclinic).

The crystal system of picene was first examined by Bernal and Crowfoot (1935); the authors obtained the sample from natural sterols, employed X-ray and optical methods, and incorrectly concluded that it is orthorhombic. Their examined samples were derived from natural sterols by cracking distillation (Ingold 1927) and contained significant impurities (Cook et al. 1934; Thompson 1935). Thus, PAH molecules other than picene might have gotten mixed into the crystal structure of the sample and misled Bernal and Crowfoot (1935) into the above-mentioned conclusion. This interpretation is consistent with those on both the crystal structure (Fig. 10) and the formation process of the present idrialite discussed in the following section.

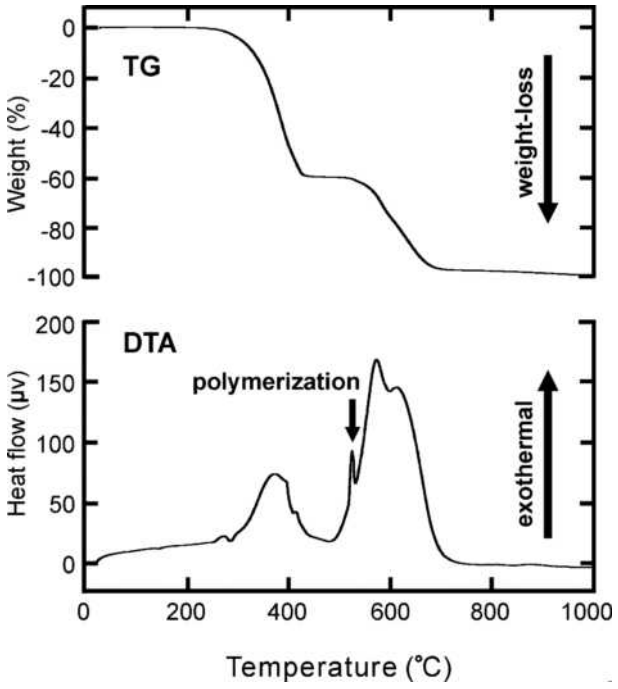

FIGURE 8. TG and DTA curves of the idrialite from Skaggs Springs.

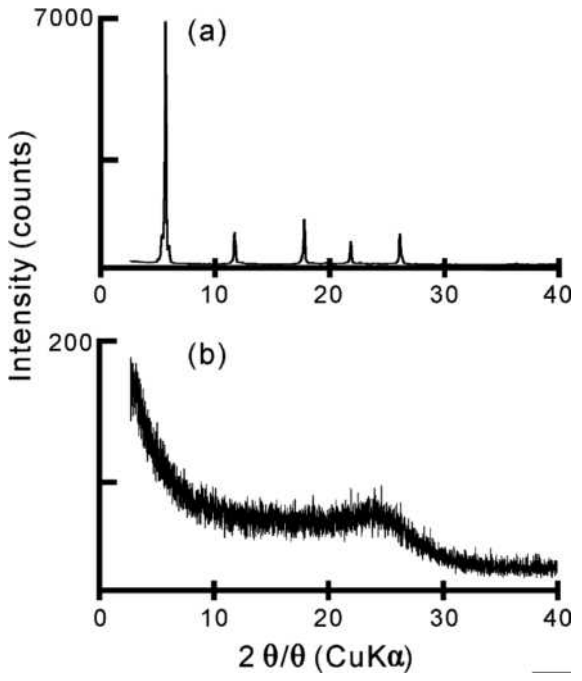

FIGURE 9. Powder X-ray diffraction patterns of (**a**) the present idrialite and (**b**) the pyrolytic residue formed by heat treatment of the above idrialite up to 500 °C.

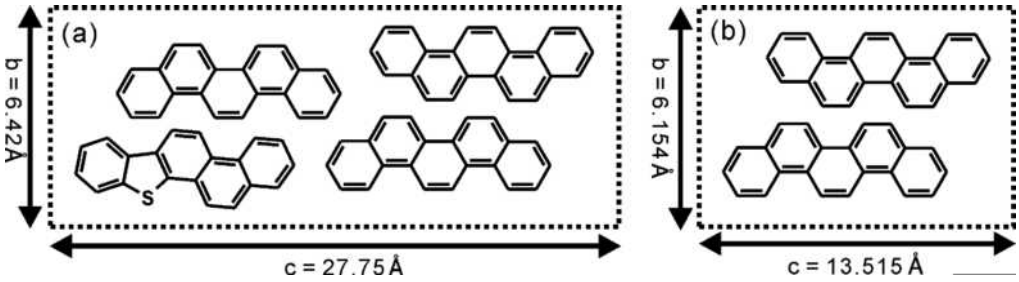

FIGURE 10. Schematic representations of the molecular arrangement in (**a**) the Skaggs Springs idrialite and (**b**) highly purified picene (De et al. 1985).

The formation process inferred from the bulk analyses

It is noteworthy that the present samples were completely volatilized up to 740 °C (Figs. 8 and 9), whereas other types of natural organic matter in solid states (e.g., coal, pitch, oil shale, and kerogen) leave carbonaceous residues on the thermal analyses up to 1000 °C (Martínez-Alonso et al. 1992; Guillén et al. 1996). On the other hand, there remains no residue when natural organic matter in liquid states (e.g., petroleum and crude oil) is completely combusted up to 640 °C (Jiang et al. 2000; Shishkin 2006). The present idrialite is more similar to liquid organic matter in thermal behavior and left no solid residue. Hence the thermal analysis suggests that the PAH mineral was crystallized from fluid phases. In addition, the paragenesis of the associated minerals in our specimen mentioned above indicates that the PAH molecules in idrialite were migrated by hydrothermal fluids.

The carbon isotopic composition of the idrialite was –24.429 ± 0.090‰ (vs. VPDB), consistent with that of the organic matter derived from plants. Higher-plant terpenoids commonly contain pentacyclic aromatic hydrocarbons (Wang and Simoneit 1990; Killops and Killops 2005) such as taraxerol (Appendix 1b) and β-amyrin (Appendix 1c). It is known that these hydrocarbons undergo aromatization (reduction of H/C-ratio) during diagenesis and convert to picene, which has been confirmed by both laboratory experiments (Hayatsu et al. 1987) and analysis of various biomarkers in sediments (Simoneit 1986). In addition, Freeman et al. (1994) concluded that the carbon isotopic fractionation hardly occurs with diagenetic aromatization. Hence the carbon isotopic composition of the present idrialite indicates that the PAH molecules composing the organic mineral have been derived from sedimentary organic matter of plant origin. This interpretation on the origin of our idrialite is consistent with that by Peabody and Einaudy (1992): all of the components of the Culver-Baer mercury deposit including cinnabar, native mercury, and petroleum may have been derived from the local sedimentary rocks and transported to the deposit in fluid phases.

Phase separation of the organic matter

The idrialite in our samples consists of hydrophobic molecules and thus intermolecular bonding between them should be due to van der Waals interactions in the same manner as found in karpatite (a natural crystal of coronene, $C_{24}H_{12}$: Echigo et al. 2007). In contrast, the brown parts (amorphous organic matter) contain hydrophilic molecules; hydrogen bonding dominates the intermolecular bonding between them (Matsubara et al. 1993; Wright 1995). The differences in intermolecular bonding between hydrophobic (idrialite) and hydrophilic (amorphous organic matter) molecules lead to their separate precipitation from the fluid by which those PAH molecules were transported. In view of the fact that the melting point of the amorphous part is much lower than that of idrialite (Grinberg and Shimanskii 1954), the idrialite should have crystallized prior to the amorphous material. Afterward, the remaining hydrophilic compounds were solidified and filled up the space between the idrialite crystals to have the characteristic texture shown in Figure 3c.

Amorphous organic matters co-existing with idrialite are reported only in the present specimens from Skaggs Springs. No amorphous component is associated with idrialite from Idrija mercury deposit (Strunz and Contag 1965), the type locality, which suggests that small PAHs are completely removed from hydrothermal fluids in the latter locality. In addition, idrialite from the latter contains more 6-ring PAHs than that from the former (Wise et al. 1986). The melting point and thermodynamic stability of PAHs are increased with the number of benzene rings (Minkin et al. 1994; Krygowski and Cyrański 2001). One inference from the above might be that idrialite from Idrija mercury was crystallized at higher temperature than that from Skaggs Springs.

ACKNOWLEDGMENTS

This investigation was supported by Research Fellowships of the Japan Society for the Promotion of Science for Young Scientists (project no. 17-7332 and no. 20-1531). Helpful comments by Jan Jehlička and an anonymous reviewer led to improvements in the manuscript. We are indebted to Barry Bickmore for handling of this manuscript.

REFERENCES CITED

Bailey, E.H. (1959) Froth veins, formed by immiscible hydrothermal fluids, in mercury deposits, California. Bulletin of the Geological Society of America, 70, 661–664.

Bernal, J.D. and Crowfoot, D. (1935) The structure of some hydrocarbons related to the sterols. Journal of the Chemical Society, 1935, 93–100.

Blumer, M. (1975) Curtisite, idrialite and pendletonite, polycyclic aromatic hydrocarbon minerals: Their composition and origin. Chemical Geology, 16, 245–256.

Cook, J.W., Hewett, C.L., Mayneord, W.V., and Roe, E. (1934) Pentacyclic aromatic hydrocarbon from cholesterol. Chemistry and Industry, 569–70.

Coplen, T.B. (1996) New guidelines for reporting stable hydrogen, carbon, and oxygen isotope-ratio data. Geochimica et Cosmochimica Acta, 60, 3359–3360.

De, A., Ghosh, R., Roychowdhury, S., and Rouchowdhury, P. (1985) Structual analysis of picene, $C_{22}H_{14}$. Acta Crystallographica, C41, 907–909.

Deines, P. (1980) The isotopic composition of reduced organic carbon. In P. Fritz and J.C. Fontes, Eds., Handbook of Environmental Isotope Geochemistry, 1, The Terrestrial Environment, A, p. 329–406. Elsevier, Amsterdam.

Dumas, J. (1832) Ueber die Verbindungenvon Wasserstoff und Kohlenstoff (Naphthalin, Paranaphthalin und Idrialin). Annalen der Physik, 102, 517–530.

Echigo, T., Kimata, M., and Maruoka, T. (2007) Crystal-chemical and carbon-

isotopic characteristics of karpatite ($C_{24}H_{12}$) from the Picacho Peak Area, San Benito County, California: evidences for the hydrothermal formation. American Mineralogist, 92, 1262–1269.
Everhart, D.L. (1950) Skaggs Springs quicksilver mine, Sonoma County, California. California Journal of Mines and Geology, 46, 385–94.
Frank, O., Jehlička, J., and Edwards, H.G.M. (2007) Raman spectroscopy as tool for the characterization of thio-polyaromatic hydrocarbons in organic minerals. Spectrochimica Acta Part A: Molecular and Biomolecular Spectroscopy, 68, 1065–1069.
Frank-Kamenetskii, V.A. and Maleeva, T.P. (1953) Curtisite from Trans-Carpathia. Doklady Akademii Nauk SSSR, 88, 135–136.
Freeman, K.H., Boreham, C.J., Summons, R.E., and Hayes, J.M. (1994) The effect of aromatization on the isotopic compositions of hydrocarbons during early diagenesis. Organic Geochemistry, 21, 1037–1049.
Gaines, R.V., Skinner, H.C.W., Foord, E.E., Mason, B., and Rosenzweig, A. (1997) Dana's New Mineralogy: the System of Mineralogy of James Dwight Dana and Edward Salisbury Dana, 8th edition, p. 1011. Wiley, New York.
Galimov, E.M. (1995) Fractionation of carbon isotopes on the way from living to fossil organic matter. In E. Wada, T. Yonegawa, M. Minagawa, T. Ando, and B.D. Fry, Eds., Stable Isotopes in the Biosphere, p. 133–170. Kyoto University Press, Japan.
Geissman, T.A., Sim, K.Y., and Murdoch, J. (1967) Organic minerals, picene and chrysene as constituents of the mineral curtisite (idrialite). Experientia, 23, 793–794.
Gold, P. (1980) Thermal analysis of exothermic processes in coal pyrolysis. Thermochimica Acta, 42, 135–152.
Grinberg, I.V. and Shimanskii, V.M. (1954) Study of the chemical nature of the colored organic mineral curtisite and its associates. Mineralogicheskii Sbornik, 8, 95–108.
Guillén, M.D., Domínguez, A., Iglesias, M.J., Fuente, E., and Blanco, C.G. (1996) Analysis of coal tar pitch: relations between thermal behaviour and composition. Fuel, 75, 1101–1107.
Harwood, L.M. and Claridge, T.D.W. (1997) Introduction to Organic Spectroscopy, p. 91. Oxford University Press, U.K.
Hayatsu, R., Botto, R.E., Scott, R.G., McBeth, R.L., and Winans, R.E. (1987) Thermal catalytic transformation of pentacyclic triterpenoids: Alteration of geochemical fossils during coalification. Organic Geochemistry, 11, 245–250.
Ingold, C.K. (1927) Organic chemistry Part II—Homocyclic division. Annual Report of the Progress of Chemistry, 24, 106–158.
Jehlička, J., Edwards, H.G.M., Jorge Villar, S.E., and Frank, O. (2006) Raman spectroscopic study of the complex aromatic mineral idrialite. Journal of Raman Spectroscopy, 37, 771–776.
Jiang, W., Tran, T., Song, X., and Kinoshita, K. (2000) Thermal and electrochemical studies of carbons for Li-ion batteries 1. Thermal analysis of petroleum and pitch cokes. Journal of Power Sources, 85, 261–268.
Killops, S. and Killops, V. (2005) Introduction to Organic Geochemistry, 2nd edition, p. 393. Blackwell Publishing, Oxford.
Kimata, M., Shimizu, M., Saito, S., Murakami, H., Ohkanda, T., and Shimoda, S. (1990) Rapid collection of the X-ray powder pattern from a single microcrystal by crystal movement of Gandolfi style. Annual Report of the Institute of Geoscience, University of Tsukuba, 16, 63–68.
Krygowski, T.M. and Cyrański, M.K. (2001) Structural aspects of aromaticity. Chemical Reviews, 101, 1385–1420.
Martínez-Alonso, A., Bermejo, J., and Tascón, J.M.D. (1992) Thermoanalytical studies of pitch pyrolysis: comparison with polycyclic aromatic hydrocarbons. Journal of Thermal Analysis, 38, 811–820.
Maruoka, T., Koeberl, C., Matsuda, J., and Syono, Y. (2003) Carbon isotope fractionation between graphite and diamond during shock experiments. Meteoritics and Planetary Science, 38, 1255–1262.
Matsubara, Y., Zhou, Z., Takekuma, S.-I., Koyama, H., and Huang, X. (1993) The crystal structure of abietic acid. Chemistry Express, 8, 237–240.
Minkin, V.I., Glukhovtsev, M.N., and Simkin, B.Y. (1994) Aromaticity and Antiaromaticity: Electronic and Structural Aspects, p. 313. Wiley, New York.
Murphy, C.B. (1970) Polymeric materials studied by DTA. In R.C. Mackenzie, Eds., Differential Thermal Analysis I, p. 643–671. Academic Press, London.
Nakata, Y., Suzuki, M., Okutani, T., Kikuchi, M., and Akiyama, T. (1989) Preparation and properties of SiO_2 from rice hulls. Journal of the Ceramic Society of Japan, 97, 842–849.
Nishida, N. and Kimata, M. (1997) Electron probe micro analysis of minerals for light elements: Carbon and nitrogen. Kobutsugaku Zasshi, 26, 203–210.
Nishida, N., Kimata, M., Kyono, A., and Hatta, T. (2003) Quantitative analysis of light elements (carbon and nitrogen) and coexisting heavy elements in minerals: Nitrogen in ammonioleucite. Recent Research Developments in Mineralogy, 3, 17–31.
Peabody, C.E. and Einaudy, M. (1992) Origin of petroleum and mercury in the Culver-Baer cinnabar deposit, Mayacmas District, California. Economic Geology, 87, 1078–1103.
Ransome, A.L. and Kellogg, J.L. (1939) Quicksilver resources in California. California Journal of Mines and Geology, 35, 353–469.
Reed, S.J.B. (1997) Electron Microprobe Analysis, 2nd edition, p. 344. Cambridge University Press, New York.
SDBS-Web (2007) Spectral Database for Organic Compounds: SDBS. National Institute of Advanced Industrial Science and Technology, date of access, http://riodb01.ibase.aist.go.jp/sdbs/.
Servos, K. (1965) Evenkite, flagstaffite, idrialite and refikite. **(In New Mineral Names, Fleischer, M., p. 2096–2111.)** American Mineralogist, 50, 2109–2110.
Sherlock, R. (2000) The association of gold-mercury mineralization and hydrocarbons in the coast ranges of northern California. In M. Glikson and M. Mastalerz, Ed., Organic Matter and Mineralization: Thermal Alternation, Hydrocarbon Generation and Role of Metallogenesis, p. 378–399. Kluwer Academic Publications, Dordrecht.
Shishkin, Y.L. (2006) Scanning calorimetry and thermogravimetry in analysis of petroleum systems. Determination of the component composition. Chemistry and Technology of Fuels and Oils, 42, 300–307.
Silverstein, R.M., Bassler, G.C., and Morrill, T.C. (1981) Spectrometric Identification of Organic Compounds, 4th edition, p. 442. Wiley, New York.
Simoneit, B.R.T. (1986) Cyclic terpenoids of the geosphere. In R.B. Johns, Ed., Biological Markers in the Sedimentary Record, p. 43–99. Elsevier, Amsterdam.
Sonibare, O.O., Ehinola, O.A., and Egashira, R. (2005) Thermal and geochemical characterization of Lokpanta oil shales, Nigeria. Energy Conversion and Management, 46, 2335–2344.
Standley, L.J. and Simoneit, B.R.T. (1994) Resin diterpenoids as tracers for biomass combustion aerosols. Journal of Atmospheric Chemistry, 18, 1–15.
Strunz, H. and Contag, B. (1965) Evenkit, flagstaffit, idrialin und reficit. Neues Jahrbuch für Mineralogie, Monatshefte, 1, 19–25.
Thompson, H.W. (1935) Is Diel's hydrocarbon "$C_{18}H_{16}$" a pure single substance? Chemistry and Industry, 1027–1028.
Vredenburgh, L.M. (1981) Tertiary gold-bearing mercury deposits of the Coast Ranges of California. California Geology, 35, 23–27.
Wakabayashi, J. (1992) Nappes, tectonics of oblique plate convergence, and metamorphic evolution related to 140 million years of continuous subduction, Franciscan Complex, California. Journal of Geology, 100, 19–40.
Wang, T.-G. and Simoneit, B.R.T. (1990) Organic geochemistry and coal petrology of Tertiary brown coal in Zhoujing Mine, Baise Basin, South China: 2. Biomarker assemblage and significance. Fuel, 69, 12–20.
Wise, S.A., Campbell, R.M., West, W.R., Lee, M.L., and Bartle, K.D. (1986) Characterization of polycyclic aromatic hydrocarbon minerals, curtisite, idrialite and pendletonite using high-performance liquid chromatography, gas chromatography, mass spectrometry, and nuclear magnetic resonance spectroscopy. Chemical Geology, 54, 339–357.
Wright, F.E. and Allen, E.T. (1930) A new organic mineral from Skaggs Springs, Sonoma County, California. American Mineralogist, 15, 169–173.
Wright, J.D. (1995) Molecular Crystals, 2nd edition, p. 221. Cambridge University Press, New York.
Zhang, Q.L. and Li, W.J. (1990) A calibrated measurement of the atomic-weight of carbon. Chinese Science Bulletin, 35, 290–296.

MANUSCRIPT RECEIVED JULY 17, 2008
MANUSCRIPT ACCEPTED MAY 15, 2009
MANUSCRIPT HANDLED BY BARRY BICKMORE

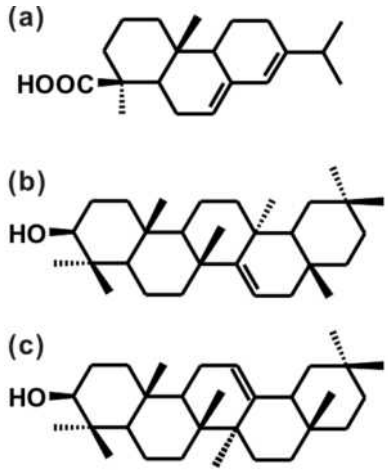

APPENDIX 1. Molecular structures of cyclic terpenoids (Simoneit 1986) referred in the text: (**a**) abietic acid, (**b**) taraxerol, and (**c**) β-amyrin.